



SKYNET

Hitoshi Irie and Teruyuki Nakajima

Contents

1	Introduction	2
2	International Collaboration Within SKYNET	2
3	Principles, Uncertainty, Calibration, and Selected Scientific Findings	3
4	Public Data Availability	7
5	Conclusions	8
	References	8

Abstract

The sky-radiometer-based observation network called SKYNET is briefly introduced. Two dedicated on-site calibration methods, the improved Langley (IL) and solar disk scan (SDS) methods, enable long-term continuous well-calibrated observation of the optical properties of atmospheric aerosols. The uncertainty in the calibration constant derived using the IL method was estimated to be better than 2.4%. The uncertainty in the solid view angle estimated using the SDS method was improved and found from simulation to be lower than 0.5% under low aerosol conditions. To confirm these estimates, aerosol optical depth (or aerosol optical thickness) comparisons with other independent data generally showed a root-mean-square difference smaller than ~ 0.02 at a wavelength (λ) ≥ 500 nm and ~ 0.03 at shorter wavelengths. The accuracy of the single scattering albedo retrieval was found to be better than ~ 0.02 for $\lambda \leq 500$ nm and tended to take a larger value of ~ 0.05 at 870 nm. Recent progress supporting the ability of SKYNET to enable precise quantitative analysis of light-absorbing aerosols is also presented. Efforts to improve the retrieval methods for aerosols and other

H. Irie (✉)

Center for Environmental Remote Sensing, Chiba University, Chiba, Japan

e-mail: hitoshi.irie@chiba-u.jp

T. Nakajima

National Institute for Environmental Studies, Ibaraki, Japan

components, such as clouds, water vapor, and ozone, are ongoing together with growth of the international SKYNET community.

Keywords

Sky radiometer · Aerosol · Network · On-site calibration · International collaboration

1 Introduction

SKYNET is a research group of sky radiometer users who formed in the early 2000s, when there was high demand for validation measurements from the Earth's surface for the Advanced Earth Observing Satellite-II (ADEOS-II) Global Imager project. It became recognized internationally during the East Asian Regional Experiment 2005 [1] conducted as part of the UNEP Atmospheric Brown Cloud project [2]. During the campaign, sky radiometers were deployed at several sites over East Asia as a ground-based aerosol observation network. Since then, users of sky radiometers and the SKYNET observation sites have continued to increase worldwide. Many observational studies of aerosols have been conducted to improve knowledge of the aerosol optical properties and to evaluate aerosol climate effects accurately. In particular, there is demand for sophisticated retrieval methods for the aerosol optical depth (AOD) (or aerosol optical thickness (AOT)) and single scattering albedo (SSA) as a unique function of ground-based aerosol observation networks. Continued effort toward improving and validating these retrieved optical properties of aerosols from ground-based networks is critical to improve the satellite remote sensing ability, the accuracy of modeling aerosol climate effects, and others. No single platform is currently capable of aerosol measurements with sufficiently low uncertainties in AOD (~ 0.02) and SSA (~ 0.02) that are needed to constrain the direct radiative effect to within $\sim 1 \text{ Wm}^{-2}$ [3]. Partly due to this issue, the estimates of radiative forcing still show large uncertainty.

2 International Collaboration Within SKYNET

Figure 1 shows the SKYNET observation sites recognized by the International SKYNET Committee (ISC) [4]. Users have established regional subnetwork groups in China, Europe, India, Japan, South Korea, Mongolia, and Southeast Asia for data analysis and formed the ISC to discuss matters regarding international collaboration. Historically, two major groups have played significant roles in regional data collection and data processing: the Centre for Environmental Remote Sensing (CEReS), Chiba University [5–8], and the European SkyNet Radiometers network (ESR) [9–11]. These subnetworks developed data collection and retrieval systems in parallel and are consequently not well unified. SKYNET was admitted as a contributing network to the World Meteorological Organization (WMO) Global

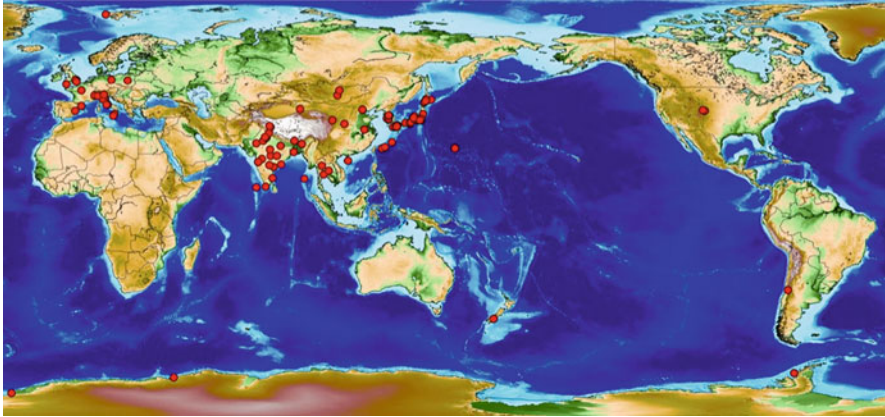


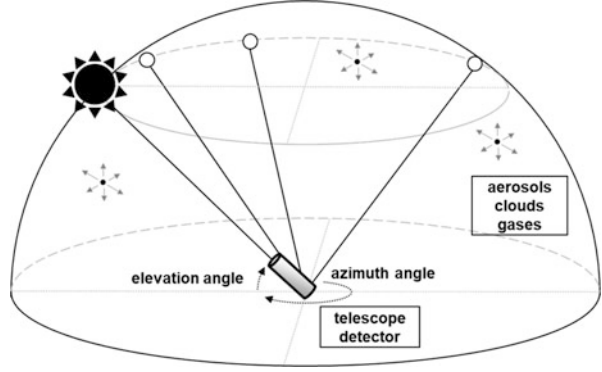
Fig. 1 A map of the SKYNET sky radiometer sites. (From Ref. [4])

Atmospheric Watch (GAW) in 2017 [4]. In this growth phase, the ISC decided to establish the International SKYNET Data Centre (ISDC) at the National Institutes for Environmental Studies in Japan, to start a shared data collection and retrieval system based on the memorandum of understanding between users and the ISDC. The ISDC provides standard products from the SKYNET network, whereas the regional subnetworks are supposed to develop improved products and new research products. Aerosol optical properties retrieved from SKYNET have been used to investigate regional and seasonal characteristics of aerosols for climate and environmental studies [8] and to validate satellite remote sensing results [12–18]. To attain these objectives, SKYNET makes observations with sky radiometers and retrieves the optical properties of aerosols, with close collaboration between national agencies, institutes, and universities.

3 Principles, Uncertainty, Calibration, and Selected Scientific Findings

All SKYNET sites are equipped with one or more sky radiometers manufactured by PREDE Co., Ltd (Fig. 2) as the main instrument. A sky radiometer is a scanning sun–sky photometer that measures direct and diffuse solar irradiance. Several versions of the sky radiometer have been developed at user requests. POM-01 is the standard version, with seven channels at 315, 400, 500, 675, 870, 940, and 1020 nm. POM-02 is an extended version equipped with additional UV channels at 340 and 380 nm and shortwave infrared wavelengths at 1600 and 2200 nm. Channels at 315 and 940 nm have been installed for atmospheric ozone and water vapor column retrieval, respectively. Full widths at half maximum of band-pass filters are 3 nm or less for channels shorter than 380 nm, 10 nm for those between 400 and 940 nm, and

Fig. 2 Schematic of the typical observation geometries of a sky radiometer



20 nm for longer wavelengths. Ship-borne observations [19] and lunar photometry [20] are possible with other versions of POM-02.

SKYNET has two dedicated on-site calibration methods for calibrating the sky radiometer without sending it to a calibration center. One is the improved Langley (IL) method for determining the calibration constant F_0 [21], which is the equivalent to the extra-terrestrial solar irradiance at a Sun–Earth distance of 1 A.U. The other is the solar disk scan (SDS) method, which determines the solid view angle (SVA) [22], which is the area on the unit sphere in the field of view of a sky radiometer.

According to Lambert-Beer’s law, the direct solar radiance measured by a sky radiometer (F) is related to the radiance at the top of the atmosphere (F_{TOA}), air mass (m), and total optical depth (τ) as:

$$\ln F = \ln F_{\text{TOA}} - m\tau \quad (1)$$

This equation can be rewritten as follows:

$$\ln F = \ln \frac{F_0}{r^2} - m\tau \quad (2)$$

$$\ln Fr^2 = \ln F_0 - m(\tau_{\text{non-aerosol}} + \tau_{\text{aerosol}}) \quad (3)$$

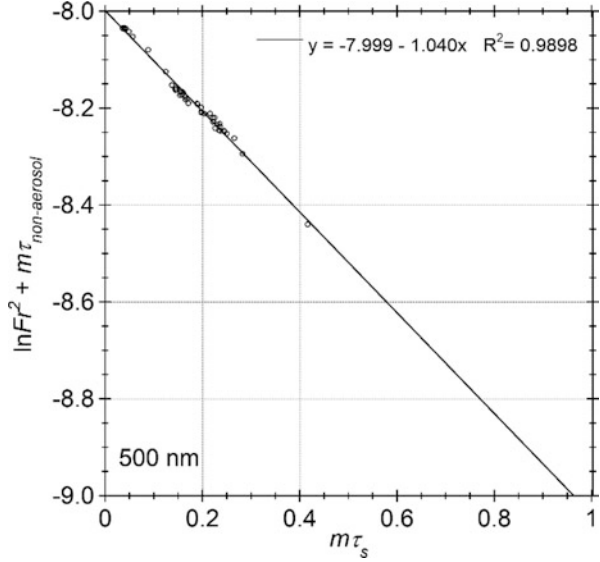
$$\ln Fr^2 = \ln F_0 - m\tau_{\text{non-aerosol}} - m\tau_{\text{aerosol}} \quad (4)$$

$$\ln Fr^2 = \ln F_0 - m\tau_{\text{non-aerosol}} - m\frac{\tau_s}{\omega} \quad (5)$$

$$\ln Fr^2 + m\tau_{\text{non-aerosol}} = \ln F_0 - \frac{1}{\omega}m\tau_s, \quad (6)$$

where r is the Sun–Earth distance, $\tau_{\text{non-aerosol}}$ is the optical depth from non-aerosol components (i.e., mainly from Rayleigh scattering and ozone), and τ_{aerosol} is the sum of the light-scattering (τ_s) and light-absorbing aerosol optical depths (τ_a).

Fig. 3 Example of the improved Langley plot for observations at Yonsei University, Seoul, Korea



For each measurement, aerosol parameters, including τ_{aerosol} , are first retrieved by inverting the data of the normalized radiance R , the ratio between the measured direct irradiance F and the measured diffuse irradiance $E(\Theta)$ within the forward-scattering range $3^\circ \leq \Theta \leq 30^\circ$, with preassigned values of the refractive index and surface albedo. This inversion uses the following equation for the radiance $L(\Theta)$:

$$L(\Theta) = \frac{E(\Theta)}{\Delta\Omega} = \omega m \tau_{\text{aerosol}} P(\Theta) F + O(\text{multiple scattering}), \quad (7)$$

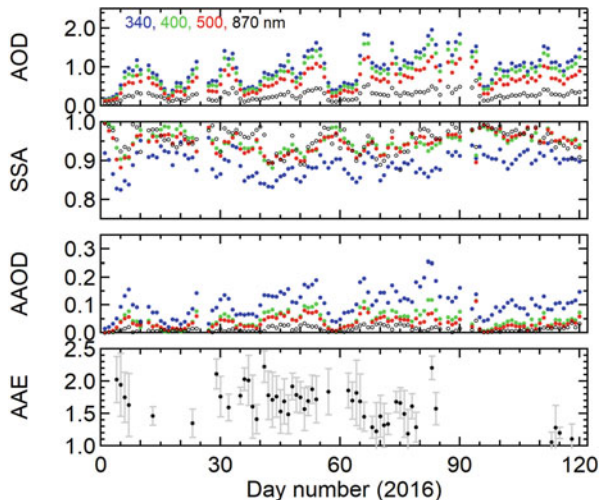
where $\Delta\Omega$ is the SVA, ω is the SSA, and $P(\Theta)$ is the normalized scattering phase function. Then, a single scattering approximation is made using the forward scattering data for a small scattering range ($3^\circ \leq \Theta \leq 30^\circ$), where the multiple-scattering term O can be neglected. To retrieve τ_{aerosol} , the inversion is performed using the ratio of the measured quantities F and $E(\Theta)$. This means that absolute values of F or $E(\Theta)$ are not needed. Therefore, information on F_0 is not needed. Note that, in this step, the retrieved τ_{aerosol} for aerosol components is not always accurate, while the optical thickness for light-scattering (τ_s) is determined more precisely. Then, plotting the left-hand side of Eq. 6 versus $m\tau_s$ (called the improved Langley plot) yields an intercept as $\ln F_0$, which determines F_0 (Fig. 3). The accuracy of F_0 derived using the IL method in this way has been estimated to be better than about 2.4% [4]. Effort is ongoing to make the IL method function under high aerosol conditions. For this, a new cross IL (XIL) method, which exchanges the roles of x and y in the regression analysis, was proposed [4].

Several methods have been proposed for the on-site estimation of the SVA of sky radiometers. These include the solar disk scan (SDS) method, point-source or lamp

scan method [8, 23], and diffuse plate method [21, 24, 25]. Of these, the SDS method is routinely used in SKYNET measurements of the SVA of the sky radiometer by scanning a circumsolar domain of $\pm 1^\circ \times \pm 1^\circ$ around the Sun at 0.1° intervals. Recently, the following three issues were identified [22] with SVA analysis using SKYRAD.pack, which was widely used in the SKYNET community. First, the data processing did not consider changes in the air mass with the solar zenith angle during the SDS measurement. In practice, however, if SDS is performed when the air mass variation is small, then the resulting error is not expected to be significant. Second, a routine correction method of subtracting the minimum value of the measured data at the widest angle from the measured data greatly affects the measurements of the scattering angle between 1° and 1.4° . This correction method will always underestimate SVA, but the solution to this problem is not straightforward. Third, the values between 1.4° and 2.5° were not extrapolated properly. Frequently, the extrapolated value does not decrease monotonically with the scattering angle. In some cases, this phenomenon partially cancels out the underestimation of the angular integral. Then using a simulation, the uncertainty in SVA was estimated to be lower than 0.5% when an AOD at 500 nm was smaller than 0.5 (with no large particles) [22]. In reality, additional uncertainty can arise due to the pointing uncertainty (particularly under strong wind conditions) during the SDS and temporal degradation in the filter conditions that could alter the focal length. Indeed, SVA derived from SDS measurements indicated that the uncertainty in SVA was less than ± 0.01 msr or $\pm 4\%$ [8]. This result is based on SVA measurements made at night using the so-called point-light-source method, by setting an Xe-lamp at a distance [23]. For more precise estimates, more experiments are needed.

Nakajima et al. [4] summarized the results of AOD comparisons with other independent data, including those from the AERONET and PFR (precision-filter radiometers) networks. The root-mean square difference (RMSD) was found to be less than ~ 0.02 for $\lambda \geq 500$ nm and takes a larger value at ~ 0.03 for shorter wavelengths in city areas, whereas mountain comparisons showed a smaller RMSD. The SKYNET SSA data were evaluated at extended UV–NIR wavelengths [26] using comparisons with those derived from a combination of the AERONET [27], MFRSR [28, 29], and Pandora [30] inversions at Yonsei University, Seoul, South Korea, during and after the Korea–United States Air Quality Study (KORUS-AQ) international field campaign in 2016 [31]. Their study provides the first comparisons of the SKYNET and MFRSR SSA retrievals at UV wavelengths. They found SSA differences of around 0.02 for $\lambda \leq 500$ nm and a larger value of 0.05 at 870 nm, similar to earlier studies [7, 32]. These demonstrated performances facilitated comparisons of independent satellite SSA retrievals in the UV from satellite observations by Ozone Monitoring Instrument (OMI) [33]. In addition, the influence of biomass burning on the SKYNET Phimai site in Thailand during the dry period in January–April 2016 was studied [8]. For this, the absorption aerosol optical depth (AAOD) and absorption Angström exponent (AAE) were estimated from SKYNET AOD and SSA data with the following equations:

Fig. 4 Time series of the aerosol optical properties (AOD, SSA, AAOD, and AAE) retrieved from sky radiometer observations at Phimai, Thailand, for the intense biomass burning period from January to April 2016. Daily means are shown. Their 1σ standard deviations are shown as error bars. The AOD, SSA, and AAOD values for different wavelengths are shown in different colors



$$\text{AAOD}(\lambda) = \text{AOD}(\lambda) \cdot [1 - \text{SSA}(\lambda)] \quad (8)$$

$$\ln [(\text{AAOD}(\lambda))] = a - \text{AAE} \cdot \ln(\lambda), \quad (9)$$

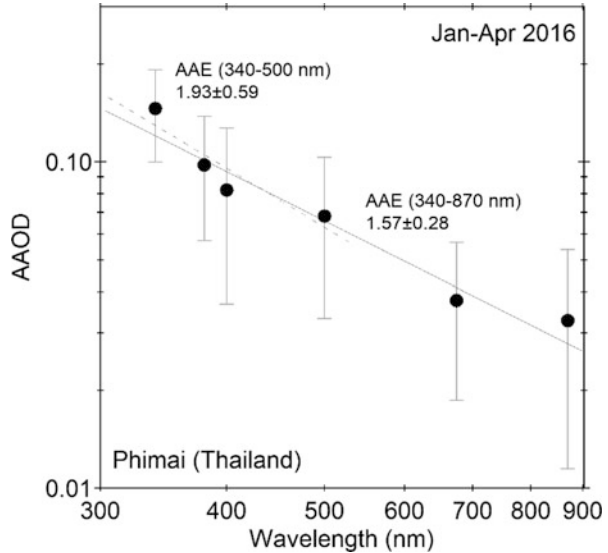
where a is the intercept.

Figure 4 shows time series of the aerosol optical properties (AOD, SSA, AAOD, and AAE) retrieved from sky radiometer observations. Reasonable correlations were found with independent collocated multi-axis differential optical absorption spectroscopy (MAX-DOAS) observations of the concentrations of trace gases originating from biomass burning (formaldehyde and glyoxal) [8]. For the period from January to April 2016, the mean estimated AAE was 1.57 ± 0.28 for all wavelengths from 340 to 870 nm (Fig. 5). For shorter wavelengths from 340 to 500 nm, the estimated mean AAE was 1.93 ± 0.59 (Fig. 5). These values were consistent with reports on biomass burning plumes. Further precise quantitative analysis of light-absorbing aerosols, particularly in biomass burning plumes, and other application research (about clouds, water vapor, and ozone) is expected to be realized in ongoing efforts to improve retrieval methods [34–36] together with a growing international SKYNET community.

4 Public Data Availability

SKYNET standard data are available publicly at the ISDC website (<http://www.skynet-isdc.org>). ISDC has two data analysis flows (SR-CEReS and ESR-MRI). For SR-CEReS, the near-real time data are publicly available as L2. For ESR-MRI, the following levels of data are available:

Fig. 5 AAOD spectrum for the period from January to April 2016. The linear least-square fitting results for 340–870 and 340–500 nm are shown by solid and dashed lines, respectively. Error bars represent the 1σ standard deviations for each wavelength



L2A: obtained using the calibration constants for the previous month. They are released at the beginning of the following day.

L2: data products obtained by reprocessing L1 data with the updated calibration constants. They are released at the end of each month, together with the calibration constant values.

5 Conclusions

The SKYNET network is briefly introduced with its dedicated on-site calibration methods, that enable long-term continuous well-calibrated observation of the optical properties of atmospheric aerosols. The uncertainties in the calibration constant derived using the IL method and the solid view angle estimated using the SDS method were small enough as demonstrated by AOD and SSA comparisons with other independent data. Further efforts to improve the retrieval methods for aerosols and other components, such as clouds, water vapor, and ozone, are ongoing together with growth of the international SKYNET community.

References

1. Nakajima T, Yoon SC, Ramanathan V, Shi GY, Takemura T, Higurashi A, Takamura T, Aoki K, Sohn BJ, Kim SW, Tsuruta H, Sugimoto N, Shimizu A, Tanimoto H, Sawa Y, Lin NH, Lee CT, Goto D, Schutgens N (2007) Overview of the Atmospheric Brown Cloud East Asian Regional Experiment 2005 and a study of the aerosol direct radiative forcing in east Asia. *J Geophys Res* 112:D24S91. <https://doi.org/10.1029/2007JD009009>

2. Ramanathan V, Li F, Ramana MV, Praveen PS, Kim D, Corrigan CE, Nguyen H, Stone EA, Schauer JJ, Carmichael GR, Adhikary B, Yoon SC (2007) Atmospheric brown clouds: hemispherical and regional variations in long range transport, absorption and radiative forcing. *J Geophys Res* 112:D22S21. <https://doi.org/10.1029/2006JD008124>
3. Sherman JP, McComiskey A (2018) Measurement-based climatology of aerosol direct radiative effect, its sensitivities, and uncertainties from a background southeast US site. *Atmos Chem Phys* 18:4131–4152. <https://doi.org/10.5194/acp-18-4131-2018>
4. Nakajima T, Campanelli M, Che H, Estellés V, Irie H, Kim S-W, Kim J, Liu D, Nishizawa T, Pandithurai G, Soni VK, Thana B, Tugisurn N-U, Aoki K, Go S, Hashimoto M, Higurashi A, Kazadzis S, Khatri P, Kouremeti N, Kudo R, Marengo F, Momoi M, Ningombam SS, Ryder CL, Uchiyama A, Yamazaki A (2020) An overview of and issues with sky radiometer technology and SKYNET. *Atmos Meas Tech* 13:4195–4218. <https://doi.org/10.5194/amt-13-4195-2020>
5. Takamura T, Nakajima T (2004) Overview of SKYNET and its activities. *Opt Pura Apl* 37: 3303–3308
6. Takamura T, Takenaka H, Cui Y, Nakajima TY, Higurashi A, Fukuda S, Kikuchi N, Nakajima T, Sato I, Pinker RT (2009) Aerosol and cloud validation system based on SKYNET observations: estimation of shortwave radiation budget using ADEOS-II/GLI data. *J Remote Sens Jpn* 29: 40–53
7. Khatri P, Takamura T, Nakajima T, Estellés V, Irie H, Kuze H, Campanelli M, Sinyuk A, Lee S-M, Sohn BJ, Pandithurai G, Kim S-W, Yoon SC, Martinez-Lozano JA, Hashimoto M, Devara PCS, Manago N (2016) Factors for inconsistent aerosol single scattering albedo between SKYNET and AERONET. *J Geophys Res Atmos* 121:1859–1877. <https://doi.org/10.1002/2015JD023976>
8. Irie H, Hoque HMS, Damiani A, Okamoto H, Fatmi AM, Khatri P, Takamura T, Jarupongsakul T (2019) Simultaneous observations by sky radiometer and MAX-DOAS for characterization of biomass burning plumes in central Thailand in January–April 2016. *Atmos Meas Tech* 12: 599–606. <https://doi.org/10.5194/amt-12-599-2019>
9. Campanelli M, Nakajima T, Olivieri B (2004) Determination of the solar calibration constant a sun-sky radiometer: proposal of an in situ procedure. *Appl Opt* 43:651–659
10. Campanelli M, Estelles V, Tomasi C, Nakajima T, Malvestuto V, Martinez-Lozano JA (2007) Application of the SKYRAD improved Langley plot method for the in situ calibration of CIMEL sun-sky radiometers. *Appl Opt* 46:2688–2702
11. Campanelli M, Estellés V, Smyth T, Tomasi C, Martinez-Lozano MP, Claxton B, Muller P, Pappalardo G, Pietruczuk A, Shanklin J, Colwell S, Wrench C, Lupi A, Mazzola M, Lanconelli C, Vitale V, Congeduti F, Dionisi D, Cardillo F, Cacciani M, Casasanta G, Nakajima T (2012) Monitoring of Eyjafjallajökull volcanic aerosol by the new European SkyNet Radiometers (ESR) network. *Atmos Environ* 48:33–45. <https://doi.org/10.1016/j.atmosenv.2011.09.070>
12. Higurashi A, Nakajima T (2002) Detection of aerosol types over the East China Sea near Japan from four-channel satellite data. *Geophys Res Lett* 29(17):1836. <https://doi.org/10.1029/2002GL015357>
13. Kim D-H, Sohn B-J, Nakajima T, Takamura T (2005) Aerosol radiative forcing over East Asia determined from ground-based solar radiation measurements. *J Geophys Res* 110:D10S22. <https://doi.org/10.1029/2004JD004678>
14. Sohn BJ, Nakajima T, Chun HW, Aoki K (2007) More absorbing dust aerosol inferred from sky radiometer measurements at Anmyeon, Korea. *J Meteorol Soc Jpn* 85:815–823
15. Pandithurai G, Takamura T, Yamaguchi J, Miyagi K, Takano T, Ishizaka Y, Dipu S, Shimizu A (2009) Aerosol effect on cloud droplet size as monitored from surface-based remote sensing over East China Sea region. *Geophys Res Lett* 36:L13805. <https://doi.org/10.1029/2009GL038451>
16. Campanelli M, Lupi A, Nakajima T, Malvestuto V, Tomasi C, Estelles V (2010) Columnar content of atmospheric water vapour from ground-based sun/sky radiometer measurements

- through a new in-situ procedure. *J Geophys Res* 115:D19304. <https://doi.org/10.1029/2009JD013211>
17. Khatri P, Takamura T, Shimizu A, Sugimoto N (2010) Spectral dependency of aerosol light-absorption over the East China Sea region. *SOLA* 6:1–4
 18. Hoque HMS, Irie H, Damiani A, Momoi M (2020) Primary evaluation of the GCOM-C aerosol products at 380 nm using ground-based sky radiometer observations. *Remote Sens* 12(16): 2661. <https://doi.org/10.3390/rs12162661>
 19. Kobayashi H, Shiobara M (2015) Development of new shipborne aureolemeter to measure the intensities of direct and scattered solar radiation on rolling and pitching vessel. In: *Proceedings of SPIE 9640, Remote Sensing of Clouds and the Atmosphere, 96401A, 1–9*. <https://doi.org/10.1117/12.2195691>
 20. Uchiyama A, Shiobara M, Kobayashi H, Matsunaga T, Yamazaki A, Inei K, Kawai K, Watanabe Y (2019) Nocturnal aerosol optical depth measurements with modified sky radiometer POM-02 using the moon as a light source. *Atmos Meas Tech* 12:6465–6488. <https://doi.org/10.5194/amt-12-6465-2019>
 21. Nakajima T, Tonna G, Rao R, Kaufman Y, Holben B (1996) Use of sky brightness measurements from ground for remote sensing of particulate polydispersions. *Appl Opt* 35:2672–2686
 22. Uchiyama A, Matsunaga T, Yamazaki A (2018) The instrument constant of sky radiometer (POM-02) – Part 2: Solid view angle. *Atmos Meas Tech* 11:5389–5402. <https://doi.org/10.5194/amt-11-5389-2018>
 23. Manago N, Khatri P, Irie H, Takamura T, Kuze H (2016) On the method of solid view angle calibration for SKYNET skyradiometers. In: *4th International SKYNET workshop, Rome, Italy, 2–4 March*
 24. Nakajima T, Tanaka M, Hayasaka T, Miyake Y, Nakanishi Y, Sasamoto K (1986) Airborne measurements of the optical stratification of aerosols in turbid atmospheres. *Appl Opt* 25: 4374–4381
 25. Boi P, Tonna G, Dalu G, Nakajima T, Olivieri B, Pompei A, Campanelli M, Rao R (1999) Calibration and data elaboration procedure for sky irradiance measurements. *Appl Opt* 38: 896–907. <https://doi.org/10.1364/AO.38.000896>
 26. Mok J, Krotkov N, Torres O, Jethva H, Li Z, Kim J, Koo J-H, Go S, Irie H, Labow G, Eck T, Holben B, Herman J, Loughman R, Spinei E, Lee SS, Khatri P, Campanelli M (2018) Comparisons of spectral aerosol absorption in Seoul, South Korea. *Atmos Meas Tech* 11: 2295–2311. <https://www.atmos-meas-tech.net/11/2295/2018/>
 27. Dubovik O, Holben B, Eck TF, Smirnov A, Kaufman YJ, King MD, Tanré D, Slutsker I (2002) Variability of absorption and optical properties of key aerosol types observed in worldwide locations. *J Geophys Res* 59:590–608
 28. Krotkov NA, Bhartia PK, Herman JR, Slusser JR, Labow G, Scott GR, Janson GT, Eck TF, Holben BN (2005a) Aerosol ultraviolet absorption experiment (2002 to 2004), part 1: ultraviolet multifilter rotating shadowband radiometer calibration and intercomparison with CIMEL sunphotometers. *Opt Eng* 44:041004. <https://doi.org/10.1117/1.1886818>
 29. Krotkov NA, Bhartia PK, Herman JR, Slusser JR, Scott GR, Labow G, Vasilkov AP, Eck TF, Dubovik O, Holben BN (2005b) Aerosol ultraviolet absorption experiment (2002 to 2004), part 2: absorption optical thickness, refractive index, and single scattering albedo. *Opt Eng* 44: 041005. <https://doi.org/10.1117/1.1886819>
 30. Herman J, Cede A, Spinei E, Mount G, Tzortziou M, Abuhassan N (2009) NO₂ column amounts from groundbased Pandora and MFDOAS spectrometers using the direct-sun DOAS technique: intercomparisons and application to OMI validation. *J Geophys Res* 114:D13307. <https://doi.org/10.1029/2009JD011848>
 31. Crawford JH, Ahn J-Y, Al-Saadi J, Chang L, Emmons LK, Kim J, Lee G, Park J-H, Park R-J, Woo JH, Song C-K, Hong J-H, Hong Y-D, Lefer BL, Lee M, Lee T, Kim S, Min K-E, Yum SS, Shin HJ, Kim Y-W, Choi J-S, Park J-S, Szykman JJ, Long RW, Jordan CE, Simpson JJ, Fried A, Dibb JE, Cho SY, Kim YP (2021) The Korea–United States Air Quality (KORUS-AQ) field study. *Elementa: Sci Anthropocene* 9(1). <https://doi.org/10.1525/elementa.2020.00163>

32. Che H, Shi G, Uchiyama A, Yamazaki A, Chen H, Goloub P, Zhang X (2008) Intercomparison between aerosol optical properties by a PREDE skyradiometer and CIMEL sunphotometer over Beijing, China. *Atmos Chem Phys* 8:3199–3214. <https://doi.org/10.5194/acp-8-3199-2008>
33. Jethva H, Torres O (2019) A comparative evaluation of Aura-OMI and SKYNET near-UV single-scattering albedo products. *Atmos Meas Tech* 12:6489–6503. <https://doi.org/10.5194/amt-12-6489-2019>
34. Khatri P, Iwabuchi H, Hayasaka T, Irie H, Takamura T, Yamazaki A, Damiani A, Letu H, Kai Q (2019) Retrieval of cloud properties from spectral zenith radiances observed by sky radiometers. *Atmos Meas Tech* 12:6037–6047. <https://doi.org/10.5194/amt-12-6037-2019>
35. Momoi M, Kudo R, Aoki K, Mori T, Miura K, Okamoto H, Irie H, Shoji Y, Uchiyama A, Ijima O, Takano M, Nakajima T (2020) Development of on-site self-calibration and retrieval methods for sky-radiometer observations of precipitable water vapor. *Atmos Meas Tech* 13:2635–2658. <https://doi.org/10.5194/amt-13-2635-2020>
36. Kudo R, Diémoz H, Estellés V, Campanelli M, Momoi M, Marengo F, Ryder CL, Ijima O, Uchiyama A, Nakashima K, Yamazaki A, Nagasawa R, Ohkawara N, Ishida H (2021) Optimal use of the Prede POM sky radiometer for aerosol, water vapor, and ozone retrievals. *Atmos Meas Tech* 14:3395–3426. <https://doi.org/10.5194/amt-14-3395-2021>